BIOCHEMICAL PHARMACOLOGY 71 (2006) 1570–1580

available at www.sciencedirect.com

SCIENCE DIRECT®

journal homepage: www.elsevier.com/locate/biochempharm

Decreased polyphenol transport across cultured intestinal cells by a salivary proline-rich protein

Kuihua Cai [a], *Ann E. Hagerman* [b], *Robert E. Minto* [b], *Anders Bennick* [a,*]

[a] *Department of Biochemistry, University of Toronto, Toronto, Ont., Canada M5S 1A8*
[b] *Department of Chemistry and Biochemistry, Miami University, Oxford, OH 45056, USA*

ARTICLE INFO

Article history:
Received 5 January 2006
Accepted 20 February 2006

Keywords:
Salivary proline-rich protein
Hydrolysable tannin
Pentagalloyl glucose
Caco-2 cells
Intestinal absorption
Flavonoid

Abbreviations:
PRP, proline-rich protein
3GG, trigalloyl glucose
4GG, tetragalloyl glucose
5GG, pentagalloyl glucose
DMEM, Dulbecco's minimum modified eagle's medium
TFA, trifluoroacetic acid
DMF, dimethylformamide
HATU, *O*-(7-azobenzotriazo-1-yl)-1,1,3,3-tetramethyl uranium hexafluorophosphate
HPLC, high performance liquid chromatography
TEER, transepithelial electric resistance
HBSS, Hank's balanced salt solution

ABSTRACT

Tannins are polyphenols commonly found in plant-derived foods. When ingested they can have various harmful effects, but salivary proline-rich proteins (PRPs) may provide protection against dietary tannins. The aim of this study was to investigate whether basic PRPs, a major family of salivary proteins, can prevent intestinal absorption of tannin. To do so it was necessary first to characterize transport of pentagalloyl glucose (5GG), a hydrolysable tannin, across cultured epithelial cells. Using human intestinal epithelial cells (Caco-2 cells) it was found that a partial degradation of 5GG occurred during transepithelial transport resulting in the presence of 5GG as well as tetra- and trigalloyl glucose and glucose in the receiving compartment. The sodium-dependent glucose transporter SGLT1 played a role in apical (mucosal) to basolateral (serosal) transport and transport in the opposite direction was dependent on the multidrug resistance-associated protein MRP2. An increased uptake from the apical compartment was seen when the basolateral receiving solution was human serum rather than a balanced salt solution. Transport both in apical–basolateral and basolateral–apical directions was reduced when 1B4, a human basic PRP, was added to the 5GG-containing medium. This decrease closely paralleled the formation of insoluble 5GG–1B4 complexes. It appears that the formation of insoluble tannin–protein complexes diminishes the uptake of 5GG and its metabolites. There is little evidence of other biological activities of basic PRPs so in contrast to other salivary proteins they may exert a biological function in the intestines.

* *Corresponding author at*: Department of Biochemistry, University of Toronto, 1 King's College Circle, Toronto, Ont., Canada M5S 1A8. Tel.: +1 416 978 8829; fax: +1 416 978 8548.
E-mail address: anders.bennick@utoronto.ca (A. Bennick).
0006-2952/$ – see front matter © 2006 Elsevier Inc. All rights reserved.
doi:10.1016/j.bcp.2006.02.013

HEPES, (*N*-2)hydroxyethylpiperazine-*N*′-2-ethanesulfonic acid
SGLT-1, sodium glucose transporter-1
MRP 2, multidrug resistance-associated protein 2

1. Introduction

In recent years there has been an increasing interest in plant polyphenols. This is to a large extent due to the antioxidant effect of flavonoids which are widely found in plant based foods and beverages and evidence that these compounds may not only provide protection against cardiovascular disease [1] but possibly also have an anticarcinogenic effect [2]. Tannins, a related group of high molecular weight polyphenols also present in food, may provide plant defense against environmental stressors, for example, by making plant leaves unpalatable to animals by their bitter astringent taste. Tannins are usually divided into condensed and hydrolysable tannins. Hydrolysable tannins, which are used in this study occur, for example, in a number of fruits including strawberries, blackberries, boysenberries, brambleberries and raspberries [3] as well as in animal feed [3]. They are also present in a number of medicinal plants used in herbal medicines and beverages [4]. Although tannins are also antioxidants, when ingested by animals they can have a number of harmful effects including decrease in growth and body weight gain [5–7], impaired absorption of calcium [8] and iron [9] as well as decreased activity of digestive enzymes [10,11]. Tannins also have other potentially harmful effects on humans. Thus cotton mill and grain elevator workers suffer from an acute inflammation of the lungs known as byssinosis [12] due to inhalation of tannin-containing dust. Tannins have in the past been used for treatment of extensive burns, but the practice was abandoned because it was found to be hepatotoxic [13]. Furthermore, tannins have also been part of Barium enemas used in intestinal radiographic examinations, but the practice was discontinued because of the hepatotoxic effect of tannin [14].

One of the characteristics of tannins is their ability to precipitate proteins, and proteins with a high content of proline are especially effective [15]. Saliva contains a group of proline-rich proteins (PRPs)* that accounts for 70% of total parotid protein [16]. Of these acidic PRPs have activities suggesting that they are important in calcium and mineral homeostasis [17,18] and glycosylated PRPs have lubricating activity [19]. The remainder known as basic PRPs constitute 23% of parotid protein [16]. Although there have been many investigations of PRPs, there is little evidence for a role of basic PRPs in the mouth, suggesting that they may be important in other organs.

In this connection it has been proposed that PRPs may constitute a first line of defense against dietary tannins [20]. This proposal is supported by experiments showing that feeding tannin to rats result in a decreased growth rate, but after a few days the growth returns to normal concomitantly with a marked stimulation of PRP synthesis [21,22]. Feeding tannin to hamsters also results in decreased growth, but in this case the growth remains retarded as long as the animals are fed tannin and there is no induction of PRP synthesis [23]. It thus appears that PRPs provide protection against tannins. Part of this protection may be related to formation of tannin–PRP complexes, which in turn may diminish intestinal uptake of tannin. In vitro studies have shown that most insoluble PRP–tannin complexes formed under conditions existing in the mouth remain insoluble when subsequently exposed to environments similar to those of the stomach and the intestines. However, a notable amount of the complexes deaggregate resulting in soluble tannins [24]. Thus it is likely that free tannin as well as protein–tannin complexes will be present in the intestines. Consequently it was decided to investigate the effect of a representative basic PRP, 1B4 on the transport of pentagalloyl glucose (5GG), a hydrolysable tannin, across human intestinal cells. Since little is known about epithelial transport of 5GG, it was necessary in the first instance to evaluate transport of 5GG across the cultured epithelial cells.

2. Materials and methods

2.1. Materials

The following supplies for tissue culture were obtained from Life Technologies, Burlington, Ont., Canada: Dulbecco's modified Eagle's Medium (DMEM), antibiotic–antimycotic solution 100× concentrated, 10 mM MEM non-essential amino acids solution and Sodium Pyruvate, 100 mM. Human serum was prepared from outdated human plasma obtained from the Hospital for Sick Children, Toronto. The plasma was clotted by adding $CaCl_2$ to a final concentration of 20 mM. The clot was removed by centrifugation at $12{,}000 \times g$ for 10 min. Fetal bovine serum was purchased from Sigma Canada Ltd., Oakville, Ont., Canada, and 12- and 6-well Costar Transwell tissue culture plates with polyester membranes from Corning Inc., Corning, NY, USA. Caco-2 cells were obtained from American Type Culture Collection, Manassas, VA, USA.

Other supplies included [^{3}H]-propranolol and [^{14}C]-mannitol (Amersham Biosciences, Bai d'Urfé, PQ, Canada) and 1,2,3,4,6-penta-*O*-galloyl-[U-^{14}C]-D-glucopyranose (5GG) with a specific activity of 8.28×10^7 or 4.51×10^8 Bq/m mol synthesized as described [25]. Thus the radioactive label is located in the glucose moiety. Unlabelled 5GG was purified as described [26]. Tri- and tetragalloyl glucose were gifts from Dr. M.P. Williamson, University of Sheffield, UK. MK-571 was the product of BIOMOL Research Laboratories Inc., Plymouth Meeting, PA, USA; verapamil, phlorizin, apolipoprotein A1, rabbit antihuman albumin antiserum, goat antirabbit IgG–peroxidase conjugate,

trifluoroacetic acid (TFA), *m*-cresol, 1,2-ethanediol, bromotrimethylsilane, thioanisole, and piperidine were obtained from Sigma Canada Ltd., Oakville, Ont., Canada. Caledon Laboratories Ltd. Georgetown, Ont., Canada were the supplier of *N*,*N*-dimethylformamide (DMF) and diethyl ether. PEG-PS resin and *O*-(7-azobenzotriazo-1-yl)-1,1,3,3-tetramethyl uranium hexafluorophosphate (HATU) were obtained from Applied Biosystems, Foster City, CA, USA. All Fmoc-amino acids were purchased from Calbiochem-Novobiochem Corp., San Diego, CA, USA. LumiGlo chemiluminescent peroxidase substrate was purchased from New England Biolabs Ltd., Pickering, Ont., Canada, and sequencing grade trypsin from Roche Diagnostics, Laval, PQ, Canada. The Human Basic Proline-rich Protein IB4 (56 residues) with the sequence SPPGKPQGPPQQEGNNPQGPPP-PAGGNPQQPQAPPAGQPQGPPRPPQGGRPSRPPQ was synthesized and purified by the Biotechnology Service Centre, University of Toronto using a Novasyn-Crystal Peptide Synthesizer (NovaBiochem Ltd, Nottingham, UK) by Fmoc-chemistry on PEG-PS resin. The solvent used throughout the synthesis was freshly purified DMF. A solution of 20% piperidine in DMF was used for removal of the Fmoc-protection groups. For each 0.5 g of resin (0.1 m mole substitution) a four-fold excess of Fmoc-amino acid activated with HATU and diisopropylethylamine (1:1:2 mol/mol/mol ratio) was used for the coupling reaction. The reaction time was 1 h at 21 °C. Following synthesis the peptide-resin conjugate was washed two times with isopropanol and another two times with diethyl ether and dried under reduced pressure. The dry peptide-resin conjugate was treated with 20 ml TFA containing 4 ml thioanisole, 0.4 ml *m*-cresole, 2 ml 1,2 ethanedithiol and 4 ml bromotrimethylsilane at 0 °C for 2 h. After removal of the resin by filtration and the TFA under reduced pressure, 50 ml of diethyl ether and 50 ml of 0.1% TFA solution was added to the residue. The aqueous layer was freeze-dried, the crude peptide dissolved in 0.1% TFA and desalted on a Sephadex G10 column. The peptide was analyzed by reverse phase HPLC on a C18 column (Phenomenex) and by mass spectroscopy on an Applied Biosystems/MDS Sciex MALDI Qstar XI, quadrupole time-of flight instrument.

2.2. Cell culture

Caco-2 cells were cultured in DMEM supplemented with 0.1 mM nonessential amino acids, 1 mM sodium pyruvate, 10% fetal bovine serum and 1% antibiotic–antimycotic solution. The cells were grown in a humidified atmosphere of 5% CO_2 at 37 °C. They were subcultured at 80% confluence.

2.3. Transport studies

Caco-2 cells were seeded in 12 mm i.d. polyester filter cell culture inserts at a density of 10^5 cells/cm^2. The basolateral (serosal) and apical (mucosal) compartments contained 1.5 and 0.5 ml culture medium, respectively. Culture medium was replaced every second day for 14 days and daily thereafter. For analysis of 5GG and its metabolites recovered from the wells 24 mm i.d. cell culture inserts were used.

For transepithelial permeability experiments cells were used 21–28 days after seeding. Transepithelial electrical resistance (TEER) of the cell layer was measured with a Millicell-ERS voltohmmeter (Millipore Ltd., Missisauga, Ont., Canada). Inserts with TEER larger than 350 Ω/cm^2 were used for transport studies. The inserts were washed with Hank's balanced salt solution (HBSS) containing 25 mM HEPES for 5 min followed by another wash for 30 min. Following removal of the wash solution and to assess the integrity of the cell monolayer, HBSS containing either [^{14}C]-mannitol or [^{3}H]-propranolol was added to the apical compartment and HBSS was added to the basolateral compartment. The plates were subsequently incubated for 1 h at 37 °C.

To measure the transepithelial transport of 5GG, following washing of the wells as described [^{14}C]-5GG in HBSS was added to either the apical or basolateral compartment. HBSS or human serum was added to the opposite side and the plates incubated for 3 h at 37 °C. At the end of incubation the TEER was measured and the amount of radionuclide transported determined by removing samples from the receiving side and counting them on a liquid scintillation counter (Beckman-Coulter, LS 6500 Multi-Purpose Scintillation Counter). In other experiments the influence of various effectors on the transport of [^{14}C]-5GG was evaluated by adding the effector alone to the second wash solution in both the apical and basolateral compartment. This was followed by adding [^{14}C]-5GG as well as the effector to either the apical or basolateral compartment and HBSS containing only the effector to the receiving side. Each experiment was done at least three times and average values calculated.

Since the proline-rich protein 1B4 forms complexes with 5GG, transport solutions containing both of these components were titurated several times to suspend evenly any insoluble complexes that might be present before counting on the liquid scintillation counter. In addition, aliquots of such transport solutions were centrifuged at 15,000 × *g* for 15 min and the resultant supernatant removed. The pellet was washed two times with HBSS, centrifuged and the washes combined with the supernatant and counted on the liquid scintillation counter. The pellet was dissolved in 10 mM triethanolamine containing 0.1% SDS and subjected to liquid scintillation counting as well. This allowed determination of the distribution of 5GG in solution and in insoluble complexes.

To evaluate the rate of transport the apparent permeability coefficient (P_{app}) was calculated using the following equation [27]:

$$P_{app}\ (\mathrm{cm\,s^{-1}}) = \frac{V}{AC_0}\frac{dC}{dt} \quad (1)$$

where V is the volume of the solution in the receiving compartment, A the membrane surface area, C_0 the initial concentration in the donor compartment and dC/dt is the change in mannitol, propranolol or 5GG concentration in the receiving solution over time. In experiments where 1B4 was added to the 5GG transport solution dC/dt rather than P_{app} was calculated since the concentration of free 5GG is not known. It was found that 5GG is metabolized during transepithelial transport, so P_{app} and dC/dt reflect the sum of transport of 5GG and its radioactive metabolites. Both parameters allow evaluation of factors that affect transepithelial transport of 5GG.

2.4. Binding of 5GG to serum proteins

As serum was the receiving solution in some transport experiments it was important to evaluate the binding of

5GG to serum proteins and the possible effect such binding would have on the transepithelial transport of 5GG. Samples of 10 μl human serum were incubated with amounts of unlabelled 5GG varying from 50 to l000 μg at 37 °C for 30 min. The samples were centrifuged at 15,000 × *g* for 5 min, the supernatants were removed, the pellets washed with 100 μl HBSS and centrifuged. The wash was repeated once and the pellet redissolved in 10 mM triethanolamine containing 0.1% SDS. Redissolved pellets containing 5 μg protein were subjected to SDS-polyacrylamide gel electrophoresis [28] on a 12.5% acrylamide gel. The gel was stained with coomassie brilliant blue.

Unstained gels were used for western blotting using rabbit antihuman albumin antiserum as the primary antibody and goat antirabbit IgG–peroxidase complex as the secondary antibody. The blot was developed with a chemiluminescent substrate according to the manufacturer's instructions.

For identification by mass spectroscopy, serum proteins precipitated by 5GG were separated by SDS-polyacrylamide gel electrophoresis as described. The band of interest was cut out of the unstained gel and subjected to reduction and alkylation followed by digestion with trypsin as described [29]. The digest was analyzed by mass spectroscopy. Saturated α-cyano-4-hydroxycinnamic acid in 70% acetonitrile containing 0.1% trifluoroacetic acid was used as the matrix solution. Spectra were obtained using MALDI MS in reflectron mode set at positive mode on an Applied Biosystems Voyager-DE STR MALDI-TOF mass spectrometer. The mass spectra were externally calibrated using a mixture of standard peptides.

To verify that the protein identified by mass spectroscopy as apolipoprotein A1 did indeed precipitate 5GG, apolipoprotein A1 or the reference proline-rich protein 1B4 were incubated with 5GG. Amounts of protein varying from 2.5 to 25 μg were incubated with 25 μg [^{14}C]-5GG in 50 μl HBSS at 37 °C for 30 min. The samples were centrifuged at 15,000 × *g* for 10 min, the supernatant removed and the pellet washed with 50 μl HBSS. This procedure was repeated once. The pellet was dissolved in 10 mM triethanolamine containing 0.1% SDS and an aliquot subjected to liquid scintillation counting.

To evaluate the nature of the compounds transported across the cells, experiments were performed with 90 μM [^{14}C]-5GG or unlabelled 5GG added on the apical side of transwells (i.d. 24 mm) and the apical and basolateral solutions from up to five wells collected at the end of the experiment were pooled and freeze-dried. The redissolved samples were analyzed by HPLC on a Beckman Ultrasphere reverse phase C18 column (4.6 mm × 25 cm) using a linear gradient from 2% acetonitrile, 0.3% formic acid to 56% acetonitrile, 0.3% formic acid over 25 min at a flow rate of 1 ml/min. The eluate was monitored by measuring A_{280}. Samples were colleted and subjected to liquid scintillation counting or analysis by mass spectroscopy as described above. The same HPLC analysis was done in experiments where the apical solution was either a mixture of 90 μM [^{14}C]-5GG and 1.2 μM 1B4 or medium without added 5GG. To evaluate transport in a basolateral to apical direction the experiments were repeated adding 10 μM [^{14}C]-5GG in the absence or presence of 10 μM 1B4 to the basolateral well.

To evaluate the stability of 5GG under the conditions of incubation 5GG was added to transwells that did not contain any cells. Aliquots of apical or basolateral solutions were removed at the end of incubation and analyzed by HPLC as described. Additional fractionations by HPLC were undertaken of pure samples of tri-, tetra- and pentagalloyl glucose to establish their elution position on the C18 column.

3. Results

Chromatography of the synthesized protein 1B4 on a C18 column showed a single symmetrical peak. The protein contained in the fraction had Mr 5589.7 as determined by mass spectroscopy, in agreement with a calculated Mr of 5589.8 for 1B4. Moreover, it was found (data not shown) that there was no difference in the precipitation of condensed tannin by purified, naturally occurring 1B4 and synthetic 1B4.

Besides using TEER measurements to evaluate the intactness of the cell layers, mannitol was used as a marker for paracellular transport and propranolol as a marker for transcellular transport. Loading 110 μM mannitol on the apical side resulted in a P_{app} of $0.44 \times 10^{-6} \pm 0.27 \times 10^{-6}$ cm/s ($n = 6$) while application of 100 μM propranolol in the apical compartment gave a P_{app} of $19.1 \times 10^{-6} \pm 6.5 \times 10^{-6}$ cm/s ($n = 5$). These values are comparable to those obtained for tight Caco-2 cell monolayers [30].

3.1. *Transport of 5GG across Caco-2 cells*

Analysis by chromatography on the C18 column of solutions that had been incubated in the absence of cells demonstrated only a prominent peak with the same elution position as 5GG (result not shown). Thus 5GG is stable during conditions of the cell transport experiments. Reversed phase chromatography on the C18 column was also used to evaluate the metabolites resulting from transport of 5GG in an apical to basolateral direction. Fig. 1A illustrates the elution pattern of the basolateral receiving solution from an experiment where unlabelled 5GG was added to the apical solution. By comparison with the elution pattern of the basolateral solution from an experiment where no 5GG was added to the apical compartment it was possible to identify the peaks that resulted from transport of 5GG and its metabolites across the cells. The peaks common to the two fractionations have been labelled with (*). The elution positions of tri-, tetra- and pentagalloyl glucose as determined by chromatography of the pure compounds are also shown in Fig. 1A. Additional identification of metabolites was obtained by mass spectroscopy. Components with masses corresponding to tri-, tetra- and pentagalloyl glucose were detected in the fractions corresponding to the elution position of these compounds. The HBSS transport solution contains 5.6 mM glucose and the elution position of glucose was also established by mass spectroscopy of the eluted fractions as shown on Fig. 1A. Additional experiments were done on apical and basolateral solutions from experiments where the apical chamber was loaded with 90 μM [^{14}C]-5GG (Fig. 1B). In the chromatogram of the apical solution (Fig. 1B, stippled line) peaks corresponding to tri-, tetra- and pentagalloyl glucose can be seen. No radioactivity was detected in the glucose elution position although the radioactive label in 5GG is located in the glucose

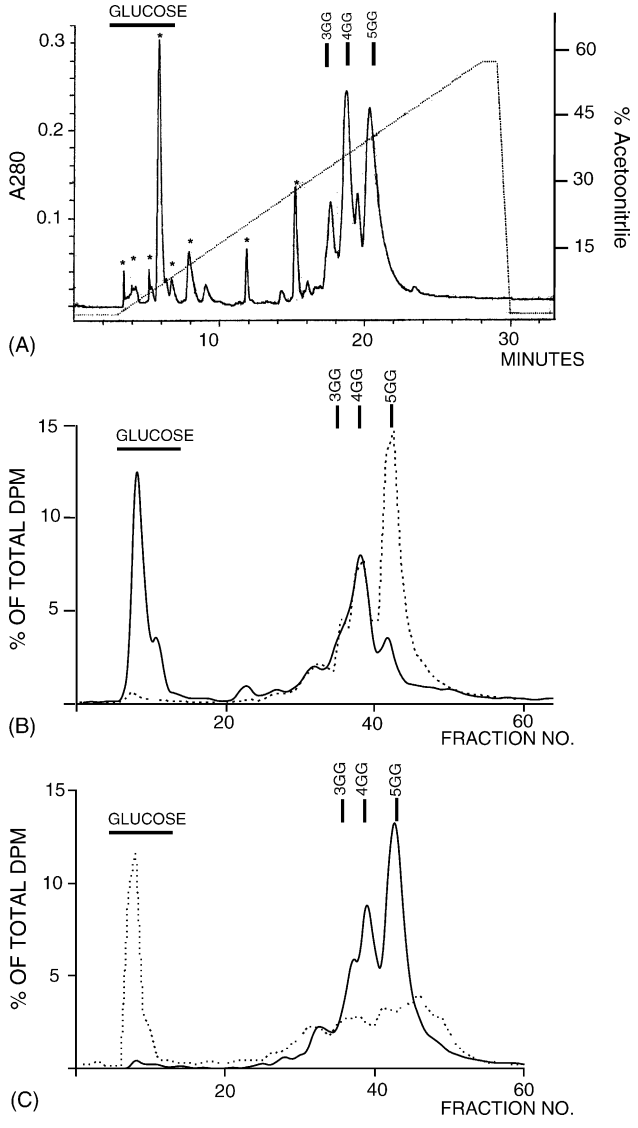

Fig. 1 – (A) Apical to basolateral transport of unlabelled 5GG. Fractionation on a C18 reverse phase column of basolateral receiving solution from an experiment in which 90 μM unlabelled 5GG had been added on the apical side of a Caco-2 cell monolayer. The stippled line shows the gradient of acetonitrile in 0.3% trifluoroacetic acid. The column was developed at a flow rate of 1 ml/min, the A_{280} of the eluate was plotted as a function of elution time and 0.5 min fractions were collected. In a parallel experiment the basolateral solution from an incubation in the absence of 5GG was fractionated under identical conditions. The (*) show peaks that are common to the two fractionations. The elution positions of trigalloyl glucose (3GG), tetragalloyl glucose (4GG) and pentagalloyl glucose (5GG) as determined by chromatography of pure compounds are shown. Mass spectroscopy of the fractions identified the elution position of glucose as shown by the horizontal bar. Moreover molecules with masses corresponding to 3GG, 4GG and 5GG were identified in fractions corresponding to the expected elution positions. (B) Apical to basolateral transport of [^{14}C]-5GG. Fractionation on the same column and under the same conditions as shown in (A). The radioactivity of each fraction was determined and the dpm of the fractions plotted as % of total dpm eluted from the column. (- - -) Apical loading solution from an experiment in which 90 μM [^{14}C]-5GG had been added to a Caco-2 cell monolayer. (—) Basolateral receiving solution from the same experiment. The elution positions of glucose, 3GG, 4GG and 5GG are shown. (C) Basolateral to apical transport of [^{14}C]-5GG. Fractionation on the same column and under the same conditions as shown in (A). The radioactivity of each fraction was determined and the dpm of the fractions plotted as % of total dpm eluted from the column. (- - -) Apical loading solution from an experiment in which 90 μM [^{14}C]-5GG had been added to a Caco-2 cell monolayer. (—) Basolateral receiving solution from the same experiment. The elution positions of glucose, 3GG, 4GG and 5GG are shown. (C) Basolateral to apical transport of [^{14}C]-5GG. Fractionation on the same column and under the same conditions as shown in (A). The radioactivity of each fraction was determined and the dpm of the fractions plotted as % of total dpm eluted from the column. (—) Basolateral loading solution from an experiment in which 10 μM [^{14}C] 5GG had been added to a Caco-2 cell monolayer. (- - -) Apical receiving solution from the same experiment. The elution positions of glucose, 3GG, 4GG and 5GG are shown.

moiety. In contrast chromatography of the basolateral solution (Fig. 1B, fully drawn line) showed radioactivity corresponding to glucose as well as tri-, tetra- and pentagalloyl glucose. When the experiment was repeated with a mixture of 5GG and 1B4 added to the apical well similar elution patterns were obtained (results not shown). Transport in a basolateral to apical direction also showed degradation of 5GG (Fig. 1C). Loading [^{14}C]-5GG into the basolateral well resulted at the end of the incubation in the presence of a mixture of radioactive compounds in the basolateral solution (Fig. 1C, fully drawn line) with elution positions corresponding to tri-, tetra- and pentagalloyl glucose but no radioactivity corresponding to glucose was seen. In the apical receiving solution radioactivity corresponding to glucose as well as tri-, tetra- and pentagalloyl glucose was noted (Fig. 1C, stippled line). The experiment was repeated adding [^{14}C]-5GG as well as 1B4 to the basolateral solution and a very similar elution pattern was obtained (results not shown).

To gain further insights into the transport of 5GG and the effect of 1B4 on this transport a series of experiment was performed in which the concentration of metabolites in the receiving compartment was estimated from the radioactivity of the samples.

Preliminary experiments demonstrated that there was a linear relationship between the amount of radioactive label transported and time within the 3 h experimental period (results not shown). Thus a 3 h incubation period was chosen.

Transport of 5GG from the apical into the basolateral compartment of the tissue culture plates was measured at [^{14}C]-5GG concentrations varying from 5 to 90 μM. From Fig. 2 it can be seen that within this range P_{app} decreases with increasing 5GG concentration as would be expected if the transport were a saturable process. To investigate the nature of the transport mechanism, apical to basolateral transport of 15 μM [^{14}C]-5GG was evaluated in the presence of concentrations of phlorizin varying from 50 to 5000 μM (Fig. 3). It is apparent from Fig. 3 that phlorizin inhibits transport of 5GG or its metabolites in a concentration dependent manner. Since phlorizin is a specific inhibitor of the sodium-dependent glucose transporter SGLT-1 [31] the results indicate a role for this transporter in apical to basolateral transport of 5GG or its metabolites across Caco-2 cells.

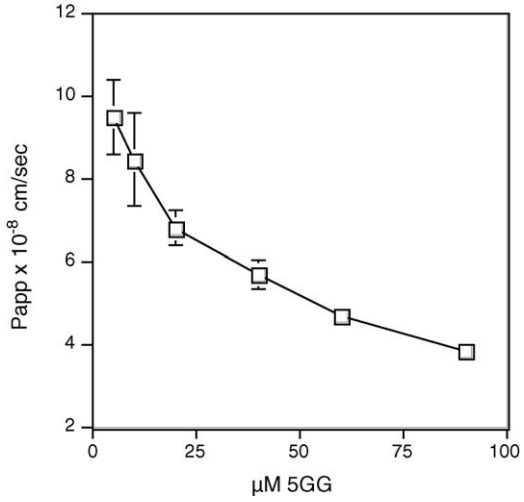

Fig. 2 – Effect of concentration of 5GG on apical to basolateral transport across Caco-2 cells. P_{app} is plotted as a function of 5GG concentration in the apical donor compartment. Mean ± S.D. of four results has been plotted. In some instances the error bar is too small to be seen.

Transport of 5GG in an apical to basolateral direction was compared with transport in the opposite direction using 10 μM [^{14}C]-5GG. Whereas, P_{app} for apical to basolateral transport was $8.4 \times 10^{-8} \pm 3.3 \times 10^{-8}$ cm/s it was $34.6 \times 10^{-8} \pm 5.7 \times 10^{-8}$ cm/s for basolateral to apical transport (six determinations). This approximately four-fold higher P_{app} for basolateral to apical transport was significantly different at the 0.01% level. Basolateral to apical transport was evaluated at concentrations of [^{14}C]-5GG varying from 2.5 to 30 μM. Within this range there was no change in P_{app} from the value obtained at 10 μM. Addition of 40 μM 5GG to the basolateral compartment caused

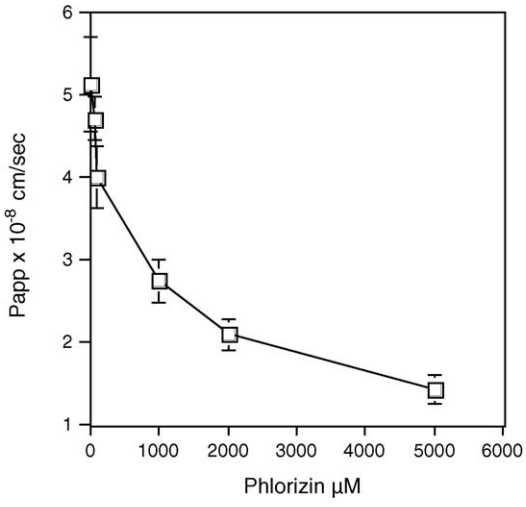

Fig. 3 – Effect of phlorizin on apical to basolateral transport of 5GG across Caco-2 cells. The apical compartment was loaded with 15 μM 5GG containing various concentrations of phlorizin. The mean P_{app} ± S.D. (n = 4) has been plotted as a function of phlorizin concentration in the apical solution.

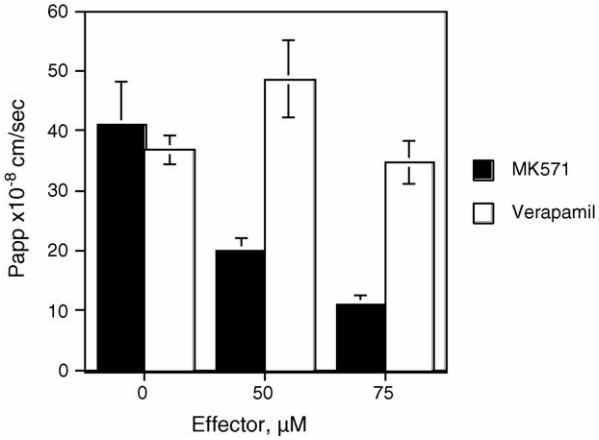

Fig. 4 – Effect of verapamil and MK571 on basolateral to apical transport of 5 μM 5GG. Means ± S.D. of 7–12 experiments are shown.

TEER to decrease below 350 Ω/cm^2 indicating that the cell layer was no longer intact, so it was not possible to measure P_{app} at higher concentrations of 5GG. Thus it cannot be excluded that P_{app} would be smaller at higher concentrations of 5GG and that transport of 5GG in a basolateral to apical direction is a saturable process. Verapamil, an inhibitor of P-glycoprotein [32] did not decrease basolateral to apical transport of [^{14}C]-5GG at concentrations of 50 and 75 μM (Fig. 4). In contrast, MK 571, an inhibitor of multidrug resistance-associated protein 2 (MRP2) [33], caused 51% and 73% reduction in P_{app} of 5GG and its metabolites when present in 50 and 75 μM concentration, respectively.

3.2. *Effect of 1B4 on apical to basolateral transport of 5GG*

3.2.1. *Transport of 5GG when the basolateral receiving solution is HBSS*

Fig. 5A illustrates the effect on dC/dt of adding 1B4 to a 90 μM [^{14}C]-5GG solution in the apical compartment. In the absence of 1B4 dC/dt was 14×10^{-7} μM/s. Addition of 1B4 caused a gradual decrease in dC/dt to a value of 4.1×10^{-7} μM/s at a 1B4 concentration of 21 μM. Increasing the 1B4 concentration to 160 μM had no additional effect on dC/dt. The distribution of soluble 5GG and 5GG bound in insoluble form to 1B4 in the apical solutions was determined (Fig. 5B). Addition of 1B4 caused precipitation of 5GG, which reached 89% of recovered 5GG in the presence of 21 μM 1B4. No additional precipitation was seen at higher concentrations of 1B4 and the decrease in dC/dt caused by the presence of 1B4 is closely mirrored in the increasing amount of insoluble 5GG in the apical compartment (Fig. 5B).

3.2.2. *Transport of 5GG when the basolateral receiving solution is human serum*

Fig. 6A shows the results obtained with a 90 μM [^{14}C]-5GG apical solution. In the absence of 1B4 dC/dt was 139×10^{-7} μM/s which was 10 times higher than when the receiving compartment contained HBSS (Fig. 5A). As in the previous experiment adding increasing amounts of 1B4 to the 5GG containing apical solution caused a gradual decrease in dC/dt until a value of

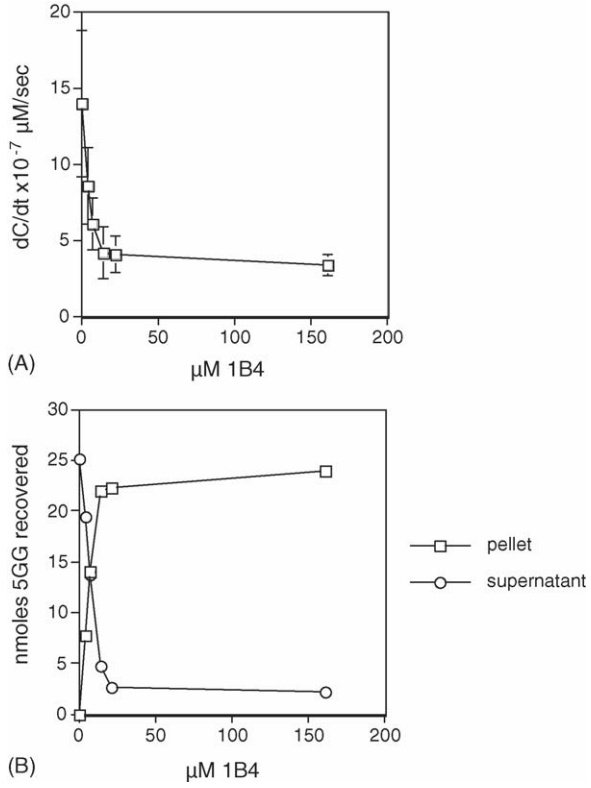

Fig. 5 – (A) The effect of the salivary PRP, 1B4 on apical to basolateral transport of 5GG across Caco-2 cells. The receiving basolateral well contained HBSS. The apical compartment was loaded with 90 µM 5GG containing various concentrations of 1B4. Mean dC/dt ± S.D. (n = 4 or 6) has been plotted as a function of 1B4 concentration. (B) Distribution of 5GG in insoluble (pellet) and soluble (supernatant) fractions in the apical loading solutions. The amount of 5GG in the two fractions is plotted as a function of the concentration of 1B4 in the loading solutions. The average values of two experiments are shown. Average recovery of 5GG was 86% of total amount initially present in the medium.

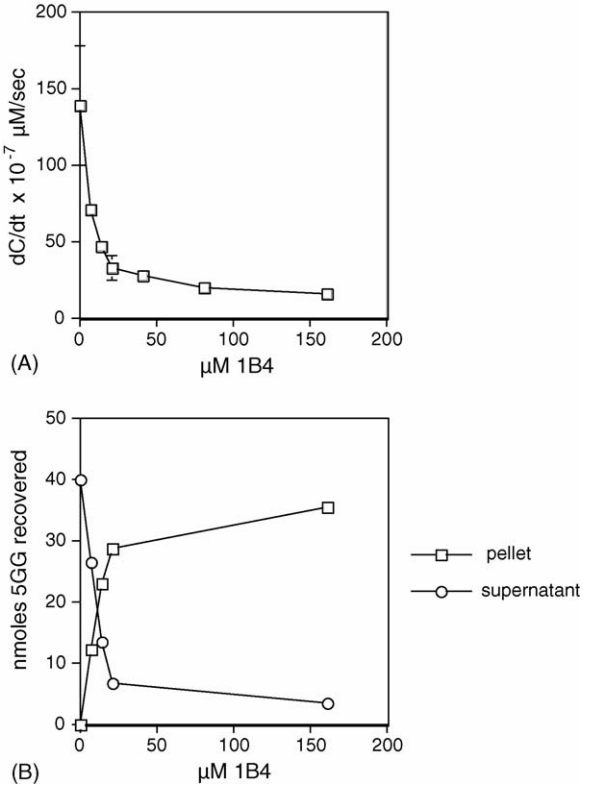

Fig. 6 – (A) The effect of the salivary PRP, 1B4 on apical to basolateral transport of 5GG across Caco-2 cells. The receiving basolateral well contained human serum. The apical compartment was loaded with 90 µM 5GG containing various concentrations of 1B4. Mean dC/dt ± S.D. (up to eight values) has been plotted as a function of 1B4 concentration. (B) Distribution of 5GG in insoluble (pellet) and soluble (supernatant) fractions in the apical loading solutions. The amount of 5GG in the two fractions is plotted as a function of the concentration of 1B4 in the loading solutions. The average values of two experiments are shown. Average recovery of 5GG was 89% of total amount initially present in the medium.

20×10^{-7} µM/s was reached in the presence of 81 µM 1B4. There was little change in dC/dt when the concentration of 1B4 was further increased. Thus even in the presence of saturating amounts of 1B4, dC/dt remains about five times larger when the receiving solution is serum rather than HBSS. From Fig. 6B it is apparent that the decrease in dC/dt upon addition of 1B4 closely paralleled the increased amount of 5GG found as insoluble complexes in the apical solution.

The increase in dC/dt when the receiving solution is serum could be due to the presence of polyphenol binding proteins since such binding would lower the concentration of free 5GG and phenolic metabolites in the serum and thus favour additional transport of polyphenols through the cell layer. Consequently precipitation of serum proteins by 5GG was investigated. As shown in Fig. 7A (lanes 1–5) addition of 5GG to serum gave rise to a precipitate, which upon analysis by gel electrophoresis showed two prominent components with Mr 67,000 and 27,000, respectively. Western blot of an acrylamide gel containing the electrophoretically separated serum protein precipitate using antiserum to albumin demonstrated strong reactivity with the 67,000 Mr band (Fig. 7B, lane 1). This is in agreement with the well-documented ability of albumin to precipitate tannins [15]. To identify the 27,000 Mr band, mass spectral analysis was undertaken. The tryptic peptide fragmentation pattern was compared with the existing protein database using the Profound and Mascot programs. The Profound program was able to match 19 of 60 peptides with apolipropotein A1 (Mr 28061). The peptides covered 63% of the sequence of this protein. The Mascot analysis also matched the tryptic peptide fragmentation pattern with apolipoprotein A1, giving a probability score of 227 with protein scores larger than 74 being significant. No other protein with a significant score was identified. It should be noted that the ratio of intensity of the apolipoprotein A1 band relative to the albumin band decreased as the amount of 5GG increased from 5 µg 5GG/µl serum (Fig. 7A, lane 1) to l00 µg 5GG/µl serum (Fig. 7A, lane 5), indicating that apolipoprotein A1 is preferentially precipitated at low 5GG concentrations.To confirm that

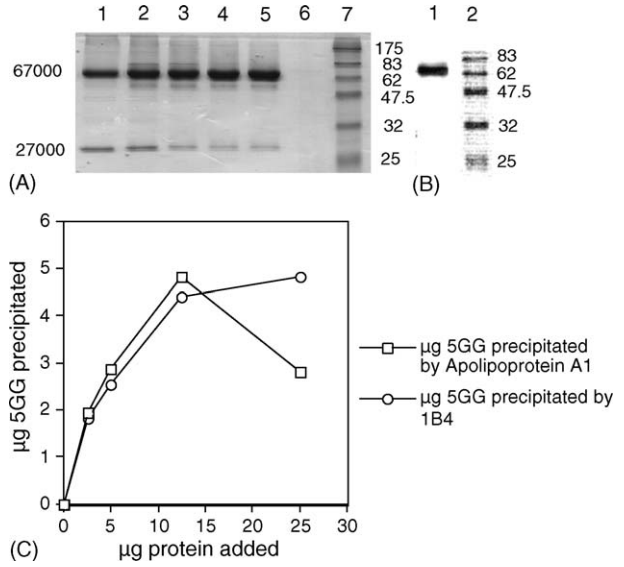

Fig. 7 – SDS-polyacrylamide gel electrophoresis of serum proteins precipitated by 5GG. (A) Gel stained with coomassie blue. The precipitates were obtained by adding the following amounts of 5GG to 10 µl human serum: Lane 1, 50 µg; lane 2, 100 µg; lane 3, 300 µg; lane 4, 600 µg; lane 5, 1000 µg, lane 6, no 5GG present. Five micrograms protein was loaded in each lane. Lane 7, molecular weight markers. (B) Western blot of gel developed with antihuman albumin antiserum. Lane 1, serum proteins precipitated by 5GG; lane 2, molecular weight markers. (C) Precipitation of 5GG by apolipoprotein A1 and 1B4. Twenty-five micrograms 5GG was incubated with varying amounts of protein and the amount of 5GG precipitated by the proteins determined. Average values of two experiments are plotted.

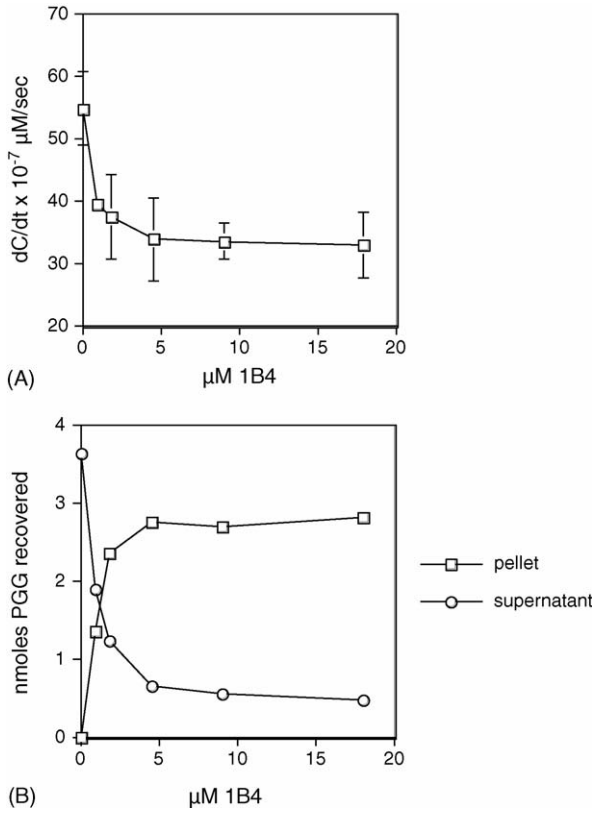

Fig. 8 – (A) The effect of the salivary PRP, 1B4 on basolateral to apical transport of 5GG across Caco-2 cells. The receiving apical well contained HBSS. The basolateral compartment was loaded with 9 µM 5GG containing various concentrations of 1B4. Mean dC/dt ± S.D. (n = 4) has been plotted as a function of 1B4 concentration. (B) Distribution of 5GG in insoluble (pellet) and soluble (supernatant) fractions in the basolateral loading solutions. The amount of 5GG in the two fractions is plotted as a function of the concentration of 1B4 in the loading solutions. Average recovery of 5GG was 73% of total amount initially present in the medium.

apolipoprotein A1 can precipitate 5GG, radioactive 5GG was incubated with either apolipoprotein A1 or 1B4. As can be seen from Fig. 7C the ability of apolipoprotein A1 to precipitate 5GG was equal to that of 1B4 up to addition of 12.5 µg protein. At higher amounts of protein the amount of 5GG precipitated by apolipoprotein A1 decreased probably due to formation of soluble protein–5GG complexes as has been observed in other studies on protein–polyphenol interaction [34].

3.3. *Effect of 1B4 on basolateral to apical transport of 5GG*

The transport of [^{14}C]-5GG across Caco-2 cells in a basolateral to apical direction is illustrated in Fig. 8A. Addition of 1B4 to the basolateral solution caused a drop in dC/dt to almost half of the value obtained in the absence of 1B4. The decrease in dC/dt closely paralleled the decrease in soluble 5GG in the basolateral solution (Fig. 8B).

4. Discussion

The harmful effects of hydrolysable tannins including 5GG are well established [5–8,13,14]. However, it is not clear how ingestion of hydrolysable tannins causes the resulting harmful effects, and it has not been established if intact or degraded hydrolysable tannins are absorbed. In this study it is shown that while 5GG can be transported across intestinal cells such as Caco-2, a large proportion of it is degraded in the process. At least part of this degradation occurs early in the transcellular transport in both apical and basolateral directions as evidenced by the presence of tri- and tetragalloyl glucose in the loading solution at the end of incubation (Fig. 1B and C). The identification of tri- and tetragalloyl glucose suggests the presence of an esterase on both the apical and basolateral sides of the cells that cleaves the bonds between the glucose and the gallic acid moieties. This conclusion is supported by the presence of carboxylesterase in brushborder membrane vesicles as well as the cell body of Caco-2 cells [35]. Since esterases are present in the intestine [36] hydrolysable tannins may be similarly cleaved in vivo. The absence of [^{14}C]-glucose from the loading solutions at the end of the experiments but presence in the receiving compartments (Fig. 1B and C) may be explained by a faster transport of glucose than gallic acid

containing metabolites. Regardless of the direction of transport a similar degradation of 5GG was observed. Since determination of [^{14}C] is used as a measure of transport the values of P_{app} and dC/dt reflect transport of all metabolites. However, P_{app} or dC/dt can still be used to measure the transport of 5GG and its metabolites. While 1B4 significantly lowers transport of 5GG and its metabolites across the cells there is little change in the pattern of metabolites detected in the receiving compartment when 1B4 is present. It has been shown that tannins inhibit digestive enzymes such as amylase and that this inhibition is relieved in the presence of PRPs [37]. Nevertheless, there was no evidence that 1B4 had a similar inhibitory effect on the cleavage of 5GG.

The P_{app} for transport of 5 μM 5GG and its metabolites in apical to basolateral direction was 9×10^{-8} cm/s (Fig. 2) a value similar to those reported for other polyphenols such as quercetin 3,4′-diglucoside, a flavonoid glucoside (P_{app} 8×10^{-8} cm/s) [30] and proanthocyanidin polymer (P_{app} 10×10^{-8} cm/s) [38]. While the P_{app} for these compounds is 1/4 of that obtained for mannitol, a marker of paracellular transport, the physiological effect of flavonoids such as quercetin glucoside is well documented [1]. While passive transport of 5GG and its metabolites into the basolateral compartment cannot be excluded, the decrease in P_{app} with increased 5GG concentration indicates that at least part of the transport occurs via a saturable mechanism and involves a carrier. The inhibition of 5GG transport into the basolateral compartment by phlorizin (Fig. 3) indicates a role of the sodium-dependent glucose transporter SGLT-1, and may reflect transport of glucose resulting from cleavage of 5GG. Inhibition of quercetin glucoside uptake in Caco-2 cells by similar concentration of phlorizin has been observed [39]. The four-fold higher P_{app} for basolateral outflow than apical uptake may contribute to the observed low P_{app} in apical to basolateral direction since 5GG and its metabolites transported into the basolateral compartment would be removed by an apically directed outflow. The difference in P_{app} also suggests that the cells have an effective mechanism for elimination of 5GG and its metabolites from the basolateral compartment. Within the experimentally possible 5GG concentration range it could not be shown that P_{app} for basolateral outflow was concentration dependent. Thus from these experiments no evidence was obtained showing that basolateral outflow of 5GG was a saturable process. This does not rule out the possibility that the transport is carrier-mediated and may simply indicate that within the experimental range of 5GG concentrations no saturation of the putative carrier took place. MRP2 has been demonstrated in the apical membrane of Caco-2 cells whereas MRP1, another member of the MRP family, is absent from the cells [40]. The observation that MK571, an inhibitor of MRP 2, inhibits outflow of 5GG and its metabolites from the basolateral compartment indicates that MRP2 indeed plays a role in a carrier-mediated transport of 5GG. In the case of quercetin glucoside evidence for a role of MRP2 in basolateral outflow has been found [40], but as observed in this study, verapamil, an inhibitor of P-glycoprotein was without inhibitory effect [40].

The observation that serum proteins form insoluble complexes with 5GG may explain the increased apical uptake of 5GG and its metabolites when serum is present in the basolateral compartment, since soluble 5GG is removed as it is transported across the Caco-2 cell layer. While it is well known that albumin precipitates tannins such as 5GG [15] there have to our knowledge been no reports of precipitation of apolipoprotein A1 by hydrolysable tannins, including 5GG although binding of (+)-catechin and procyanidins to apolipoprotein A1 has been demonstrated [41]. From Fig. 7 it can be calculated that 1 molecule of apolipoprotein A1 (Mr 28,062) maximally binds 11–12 molecules of 5GG (Mr 940), suggesting that binding of 5GG occurs at many sites on apolipoprotein A1. On a w/w ratio apolipoprotein A1 is optimally as effective as the salivary proline-rich protein 1B4 in precipitating 5GG (Fig. 7C).

The effect of serum proteins on 5GG transport also shows that any 5GG-binding protein that is present in the intestinal subepithelial compartment may increase uptake of 5GG, a factor that will be important in understanding uptake of 5GG in vivo. 1B4 shows structural characteristics typical of proteins that are effective precipitators of tannin, being intrinsically unstructured and with a high content of proline [42,43]. In contrast apolipoprotein A1 with a low content of proline has a 47 residue N-terminal globular domain followed by amphipathic α-helices (residues 49–243) [44]. The nature of interaction of 5GG with apolipoprotein A1 remains to be determined, but the structure suggests that it is fundamentally different from that observed for other proteins that effectively precipitates tannin [26,45]. Apolipoprotein A1 plays a number of biologically important roles [44], and it will be interesting to determine to what extent binding of 5GG interferes with these various functions since it may elucidate how 5GG exerts its biological effects.

If 1B4 is added to the 5GG containing transport medium dC/dt is decreased both in apical–basolateral and basolateral–apical directions (Figs. 5A, 6A and 8A) regardless of whether the receiving solution is HBSS or human serum. The highest reduction is seen in an apical to basolateral direction when serum is the receiving solution. In that case 1B4 caused maximally eight to nine-fold reduction in dC/dt (Fig. 6A). The decreases in dC/dt closely parallel increases in insoluble 5GG in the donor compartment suggesting that formation of 5GG–protein complexes contributes to the decrease in intestinal absorption of 5GG and its metabolites. Similarly the presence of any 5GG binding protein in the intestinal subepithelial compartment as exemplified by 1B4 would decrease the efflux of 5GG (Fig. 8A). The observation that 1B4 does not alter the pattern of transported metabolites suggests that it has little differential effect on cellular transport of the compounds. Taken together it appears that basic PRPs act by forming complexes with hydrolysable tannins and thereby decreasing their transcellular transport. These results, together with other studies showing limited evidence for functions of basic PRPs in the mouth but ability to provide intestinal protection by complex formation with tannins, suggest that a major biological effect of these salivary proteins occurs in the intestines [21–24,46].

While intestinal absorption of dietary tannins may be undesirable, present evidence indicates that benefits are derived from related dietary flavonoids. Whether salivary proteins affect intestinal absorption of flavonoids remains to be determined. Experimental evidence indicates that there is

only weak binding of epicatechin, a flavonoid found in tea, to PRPs [46] and little tendency for histatins, another group of effective tannin-binding salivary proteins, to form insoluble complexes with epigallocatechin gallate, a prominent tea flavonoid [26]. Thus salivary proteins may have little effect on intestinal absorption of flavonoids and exploitation of their beneficial properties in the organism at the same time as they impede absorption of the related tannins with their associated potentially harmful effects.

Acknowledgement

This work was supported by grant #36530 from the Canadian Institutes for Health Research to AB.

REFERENCES

[1] Knekt P, Järvinen R, Reunanen A, Jouni A. Flavonoid intake and coronary mortality in Finland: a cohort study. Brit Med J 1996;312:478–81.
[2] Knekt P, Järvinen R, Seppänen R, Heliövaara M, Teppo L, Pukkala E, et al. Dietary flavonoids and the risk of lung cancer and other malignant noeplasms. Am J Epidem 1997;146:223–30.
[3] Foo LY, Porter LJ. The structure of tannins of some edible foods. J Sci Food Agric 1981;32:711–6.
[4] Haslam E. Practical polyphenolics. From structure to molecular recognition and physiological action. Cambridge, UK: Cambridge University Press; 1998. p. 299.
[5] Joslyn MA, Glick Z. Comparative effects of gallotannic acid and related phenolics on the growth of rat. J Nutr 1969;98:119–26.
[6] Jambunathan R, Mertz ET. Relationship between tannin levels, rat growth and distribution of proteins in sorghum. J Agric Food Chem 1973;21:692–6.
[7] Featherstone WR, Rogler JC. Influence of tannins on the utilization of sorghum grain by rats and chicks. Nutr Rep Int 1975;11:491–7.
[8] Mitjavila S, Lacombe C, Carrera G, Derache R. Tannic acid and oxidised tannic acid on the functional state of rat intestinal epithelium. J Nutr 1977;107:2113–21.
[9] Brune M, Rossander L, Hallberg L. Iron absorption and phenolic compounds: importance of different phenolic structures. Eur J Clin Nutr 1989;43:547–57.
[10] Griffiths WD. The inhibition of digestive enzymes by polyphenolic compounds. Adv Exp Med Biol 1986;199:509–16.
[11] Horigome T, Kumar R, Okamoto K. Effects of condensed tannins prepared from leaves of fodder plants on digestive enzymes in vitro and in the intestine of rats. Brit J Nutr 1988;60:275–85.
[12] Cotes JE, Steel J, Leathart GL. Work-related lung disorders. Oxford, UK: Blackwell Scientific Publishers; 1987. p. 309–19.
[13] Erb IH, Morgan EM, Farmer EW. The Pathology of burns. The pathologic picture as revealed at autopsy in a series of 61 fatal cases treated at the hospital for sick children, Toronto, Canada. Ann Surg 1943;117:234–55.
[14] Lucke HH, Hodge KE, Patt NL. Fatal liver damage after barium enemas containing tannic acid. Can Med Assoc J 1963;89:1111–3.
[15] Hagerman AE, Butler LG. The specificity of proanthocyanidin–protein interactions. J Biol Chem 1981;256:4494–7.
[16] Kauffman DL, Keller PJ. The basic proline-rich proteins in human parotid saliva from a single subject. Arch Oral Biol 1979;24:249–56.
[17] Hay DI, Moreno EC, Schlesinger DH. Phosphoprotein inhibitors of calcium phosphate precipitation in human saliva. Inorg Pespec Biol Med 1979;2:271–85.
[18] Bennick A, McLaughlin AC, Grey AA, Madapallimattam G. The location and nature of calcium-binding sites in salivary acidic proline-rich proteins. J Biol Chem 1981;25:4741–6.
[19] Hatton MN, Loomis RE, Levine MJ, Tabak LA. Masticatory lubrication. The role of carbohydrate in the lubricating property of a salivary glycoprotein–albumin complex. Biochem J 1985;230:817–20.
[20] Mehansho H, Butler LG, Carlson DM. Dietary tannins and salivary proline-rich proteins: interactions, induction and defense mechanisms. Ann Rev Nutr 1987;7:423–40.
[21] Mehansho H, Hagerman A, Clements S, Butler LG, Rogler JC, Carlson DM. Modulation of proline-rich protein biosynthesis in rat parotid glands by sorghums with high tannin levels. Proc Natl Acad Sci 1983;80:3948–52.
[22] Mehansho H, Clements S, Sheares BT, Smith S, Carlson DM. Induction of proline-rich glycoprotein synthesis in mouse salivary glands by isoproterenol and by tannins. J Biol Chem 1985;260:4418–23.
[23] Mehansho H, Ann DK, Butler LG, Rogler J, Carlson DM. Induction of proline-rich proteins in hamster salivary glands by isoproterenol treatment and an unusual growth inhibition by tannins. J Biol Chem 1987;262:12344–50.
[24] Lu Y, Bennick A. Interaction of tannin with human salivary proline-rich proteins. Arch Oral Biol 1998;43:717–28.
[25] Chen Y, Hagerman AE, Minto RE. Preparation of 1,2,3,4,6-penta-*O*-galloyl-[U-^{14}C]-D-glucopyranose. J Label Compd Radiopharm 2003;46:99–105.
[26] Wroblewski K, Muhandiram R, Chakrabarrty A, Bennick A. The molecular interaction of human salivary histatins with polyphenolic compounds. Eur J Biochem 2001;262:428–37.
[27] Artursson P. Epithelial transport of drugs in cell culture. 1. A model for studying the passive diffusion of drugs over intestinal absorptive (Caco-2) cell. J Pharm Sci 1990;79:476–82.
[28] Laemmli UK. Cleavage of structural proteins during the assembly of the head of bacteriophage T4. Nature 1970;227:680–5.
[29] Shevchenko A, Wilm M, Worm O, Mann M. Mass spectrometric sequencing of proteins silver-stained polyacrylamide gels. Anal Chem 1996;68:850–8.
[30] Walgren RA, Walle UK, Walle T. Transport of quercetin and its glucosides across human intestinal epithelial Caco-2 cells. Biochem Pharmacol 1998;55:1721–7.
[31] Toggenburger G, Kessler M, Semenza G. Phlorizin as a probe of the small-intestinal Na^+, D-glucose cotransporter. A model. Biochim Biophys Acta 1982;688:557–71.
[32] Cornwell MM, Pastan I, Gottesman MM. Certain calcium channel blockers bind specifically to multidrug-resistant human KB carcinoma membrane vesicles and inhibit drug binding to *P*-glycoprotein. J Biol Chem 1987;262:2166–70.
[33] Gekeler V, Ise W, Sanders KH, Ulrich WR, Beck J. The leukotriene LTD4 receptor antagonist MK571 specifically modulates MRP associated multidrug resistance. Biochem Biophys Res Commun 1995;208:345–52.
[34] Hagerman AE, Robbins CT. Implication of soluble tannin–protein complexes for tannin analysis and plant defence mechanisms. J Chem Ecol 1987;13:1243–59.
[35] Imai T, Imoto M, Sakamoto H, Hashimoto M. Identification of esterases expressed in Caco-2 cells and effects of their hydrolyzing activity in predicting human intestinal absorption. Drug Metab Dispos 2005;33:1185–90.
[36] Satoh T, Taylor P, Bosron WF, Sanghan P, Hosokawa M, Du BN. Current progress on esterases: from molecular structure to function. Drug Metab Dispos 2002;30:488–93.

[37] Yan Q, Bennick A. Identification of histatins as tannin-binding proteins. Biochem J 1995;311: 341–7.
[38] Deprez S, Mila A, Huneau JF, Tome D, Scalbert A. Transport of proanthocyanidin dimer, trimer, and polymer across monolayers of human intestinal epithelial Caco-2 cells. Antioxid Redox Signal 2001;3:957–67.
[39] Walgren AA, Jiann-Trzuo L, Kinne RK-H, Walle T. Cellular uptake of dietary flavonoid quercetin 4′-β-glucoside by sodium-dependent glucose transporter SGLT1. J Pharmacol Exp Ther 2000;294:837–43.
[40] Walgren RA, Karnaky Jr KJ, Lindenmayer GE, Walle T. Efflux of dietary flavonoid quercetin 4′-β-glucoside across human intestinal Caco-2 cell monolayers by apical multidrug resistance-associated protein-2. J Pharmacol Exp Ther 2000;294:830–6.
[41] Brunet MJ, Bladé C, Salvadó J, Arola L. Human Apo A-1 and rat transferrin are the principal plasma proteins that bind wine cathecins. J Agric Food Chem 2002;50: 2708–12.
[42] Murray NJ, Williamson MP. Conformational study of a salivary proline-rich protein repeat sequence. Eur J Biochem 1994;219:915–21.
[43] Bennick A. Interaction of plant polyphenols with salivary proteins. Crit Rev Oral Biol Med 2002;13:184–96.
[44] Brouillette CG, Anantharamaiah GM, Engler JA, Borhani DW. Structural models of apolipoprotein A-1: a critical analysis and review. Biochim Biophys Acta 2001;1531:4–46.
[45] Murray NJ, Williamson MR, Lilley TH, Haslam E. Study of the interaction between salivary proline-rich proteins and a polyphenol by 1H NMR spectroscopy. Eur J Biochem 1994;219:923–35.
[46] Baxter NJ, Lilley TH, Haslam E, Williamson MP. Multiple interactions between polyphenols and a salivary proline-rich protein repeat result in complexation and precipitation. Biochemistry 1997;36:5566–77.